WAGENINGEN **UR**

For quality of life

Energy consumption and constant current operation in membrane capacitive deionization

Zhao, R., Biesheuvel, P.M., & Van der Wal, A.

Please cite this publication as follows:

Zhao, R., Biesheuvel, P.M., & Van der Wal, A. (2012). Energy consumption and constant current operation in membrane capacitive deionization. Energy & Environmental Science, 5(11), 9520.

You can download the published version at:

http://dx.doi.org/10.1039/C2EE21737F

Energy Consumption and Constant Current Operation in Membrane Capacitive Deionization

R. Zhao,[1,2] P.M.Biesheuvel[1,2,*] and A. van der Wal[1,3]

[1]*Department of Environmental Technology, Wageningen University, Bornse Weilanden 9, 6708 WG Wageningen, The Netherlands.* [2]*Wetsus, centre of excellence for sustainable water technology, Agora 1, 8900 CC Leeuwarden, The Netherlands.* [3]*Voltea B.V., Wasbeekerlaan 24, 2171 AE Sassenheim, The Netherlands. e-mail:* maarten.biesheuvel@wetsus.nl*.*

General interest paragraph (max 200 words)

Energy-efficient water desalination is essential for the economical use of groundwater and other water resources for industry, agriculture, human consumption and household applications. Here, an extensive data set is presented for the energy consumption of a novel water desalination technology, called membrane capacitive deionization (MCDI). This data set is an essential tool to assess the economic viability of MCDI. Also, we introduce an improved operation mode of MCDI in which freshwater of a constant salt concentration is produced, i.e., unvarying in time. The salt level in the produced freshwater can be tuned precisely using the electrical current and water flow rate as direct control parameters.

Abstract

Membrane capacitive deionization (MCDI) is a water desalination technology based on applying a cell voltage between two oppositely placed porous electrodes sandwiching a spacer channel that transports the water to be desalinated. In the salt removal step, ions are adsorbed at the carbon-water interface within the micropores inside the porous electrodes. After the electrodes reach a certain adsorption capacity, the cell voltage is reduced or even reversed, which leads to ion release from the electrodes and a concentrated salt solution in the spacer channel, which is flushed out, after which the cycle can start over again. Ion-exchange membranes are positioned in front of each porous electrode which has the advantage that co-ions are prevented from leaving the electrode region during ion adsorption, while also allowing for ion desorption at reversed voltage. Both effects significantly increase the salt removal capacity of the system per cycle.

The classical operation mode of MCDI at a constant cell voltage results in an effluent stream of desalinated water of which the salt concentration varies with time. In this paper, we propose a different operational mode for MCDI, whereby desalination is driven by a constant electrical current, which leads to a constant salt concentration in the desalinated stream over long periods of time. Furthermore, we show how the salt concentration of the desalinated stream can be accurately adjusted to a certain setpoint, by either varying the electrical current level and/or the water flowrate.

Finally, we present an extensive data set for the energy requirements of MCDI, both for operation at constant voltage, and at constant current, and in both cases also for the related technology in which membranes are not included (CDI). We find consistently that in MCDI the energy consumption per mole of salt removed is lower than in CDI. Within the range 10-200 mM ionic strength of the water to be

treated, we find for MCDI a constant energy consumption of ~22 kT per ion removed. Results in this work are an essential tool to evaluate the economic viability of MCDI for the treatment of saltwater.

Introduction

Access to freshwater at moderate costs is essential for direct consumption, in many household applications, and in agriculture and industry [1-7]. With the continuing growth of the human population and the increase in per capita water use, new sources of freshwater must be made available. Water desalination of brackish water, such as groundwater, is one potential solution. For energy-efficient water desalination of these water sources of relatively low salt concentration, e.g. below 5,000 ppm salt (<100 mM), instead of producing freshwater by evaporation (distillation), or by water-permeable membranes (reverse osmosis), where pure water is separated from the saline water, it may be advantageous to remove the relatively few salt molecules from the saline water and produce freshwater in this manner. This is the approach followed in electrodialysis [8], water desalination using nanochannels [9], batteries [10] microbial desalination cells [11] and wires [12], as well as in capacitive deionization (CDI) and membrane capacitive deionization (MCDI). In this manuscript we focus on CDI [2,13-40] and MCDI [41-49]. CDI also goes under the names of electrosorption desalination [15] and capacitive desalination [50].

Water desalination by CDI is a technology related to energy storage using supercapacitors [51,52,53], but with distinct differences. In CDI, by applying a cell voltage between two oppositely positioned porous electrodes, ions in the water flowing through a transport channel in between the electrodes are removed and stored in the electrical double layers (EDLs) in the micropores of the electrodes. This is the ion removal-, ion adsorption-, or charging-step. During this step, anions are adsorbed in the anode (electrode of positive polarity) and cations are stored in the cathode. After some time, the cell voltage is reduced or even reversed and the previously stored ions are released (ion release, ion desorption, discharge-step) and flushed out of the transport channel, after which a new cycle can start. Membrane Capacitive Deionization (MCDI) is a modification of CDI by placing ion exchange membranes in front of each electrode. Specifically, an anion exchange membrane is placed in front of the anode, and a cation exchange membrane is placed in front of the cathode (Fig. 1).

Because of the use of ion exchange membranes, MCDI has two major advantages over conventional CDI [43,48]. First of all, in MCDI, the co-ions that are expelled from the micropores during charging are inhibited from leaving the electrode structure. [Note that the co-ion is defined as the ion of the same charge as the electrode charge and is the ion that is repelled out of the electrode. The counterions are those of opposite charge sign to that of the surface and are attracted into the electrode. Thus a cation is the counterion in the cathode and the co-ion in the anode.] One may wonder how co-ions can be present behind the membrane (within the electrode structure) in the first place. The answer is that the membranes are slightly leaky to co-ions, and thus after several cycles, whatever the initial salt concentration behind the membrane, a certain steady-state amount of co-ions is found. In comparison, in CDI the co-ions are released from the electrodes, and end up in the spacer channel. This leads to a reduced charge efficiency of the system, i.e., per amount of transported charge, a lower number of salt molecules is removed from the water [20,27,54]. In MCDI, the co-ions expelled from the

micropores end up in the large transport pores, also called macropores, which are within the electrode structure, see Fig. 2. In order to maintain electroneutrality in the macropores, additional counterions are being transported through the membrane and stored in the macropores of the electrodes. As a consequence, during the ion removal-step, the salt concentration can become much higher in the macropores than in the spacer channel, and therefore in MCDI the macropores serve as a reservoir for ion storage [48]. In comparison, in CDI, i.e., without membranes, the salt concentration in the macropores is, during ion adsorption, just as high as that in the spacer channel, or even lower [55,56]. A second advantage of MCDI is that the cell voltage between the two electrodes can be reversed during ion desorption, which leads to a shorter duration of the discharge step and more release of counterions from the electrode [43,45,48], and thus an increase of the salt adsorption capacity of the cell in the next cycle.

At present, it is common practice to control the desalination cycles of (M)CDI by applying a constant cell voltage (the electrical potential difference between the two porous electrodes) during charging (ion adsorption) and during discharging (ion desorption) of the electrodes. For example, during ion adsorption, a typical value of V_{cell}=1.2 V is applied to adsorb ions and produce freshwater, while during discharge, the two electrodes can be short-circuited, i.e., the cell voltage is reduced to 0 V. However, operation at a constant cell voltage has as a disadvantage that the effluent salt concentration changes in time, i.e., the ion concentration in the desalinated water stream (freshwater) changes during the ion removal step. This is because at the start of the adsorption step, the EDLs are still mainly uncharged, and thus the driving force over the channel is at a maximum (no loss of cell voltage in the EDLs). Consequently, there is a large ion flux directed into the electrodes. As ion adsorption in the EDLs progresses, the EDL voltage gradually increases and the remaining voltage across the spacer channel steadily decreases in time. The overall effect is that the effluent salt concentration will first decrease, go through a minimum, and then gradually increase again. This gradual change of effluent concentration over time may not be desired in practical applications; instead, it may be more advantageous if water is produced of a constant desalination level.

To obtain freshwater with a constant reduced salt concentration, we propose a different mode to carry out the MCDI desalination cycles, namely by applying a constant current (CC) running between the two electrodes, instead of using a constant cell voltage (CV). The externally applied constant electron current, I, translates into an equally large ionic current in the cell, which has contributions from the ionic flux of positive ions (such as Na^+) and negative ions (such as Cl^-). As we will show, in MCDI, operation with constant current results in an effluent salt concentration which is constant in time, both during the ion adsorption step and during the ion desorption-step. Another advantage of operation using constant current is that the effluent concentration can be easily and accurately controlled at a certain required value by varying the current level. This may be advantageous from the viewpoint of the consumer who desires a supply of freshwater with constant and tunable salt concentration.

Furthermore, we present an extensive data set for the energy requirement of MCDI versus CDI, not only for the novel operational mode of CC, but also for the classical CV-mode of operation. These data can be used to assess the economic viability of the technology, as well as to validate process models; models which are an essential tool for the design and optimization of CDI and MCDI. We show that the

energy requirement is closely linked to the dynamic charge efficiency, an important operational parameter both in CDI and MCDI.

Experimental Section

Experimental setup

Our experimental setup [21,27,37,38,48,57,58] consists of a stack of $N=8$ parallel cells. Each MCDI cell consists of one spacer, two membranes, two electrodes, and two current collectors, which are connected to the external electrical circuit. Materials used are graphite current collectors, porous carbon electrodes (Materials & Methods, PACMM^{TM} 203, Irvine, CA, $\delta_e=362$ μm, $m_{tot}=10.75$ g total mass in the stack), anion and cation exchange membranes (Neosepta AMX, $\delta_{mem}=140$ μm, and Neosepta CMX, $\delta_{mem}=170$ μm, Tokuyama, Japan), and a polymer spacer (Glass fibre prefilter, Millipore, Ireland, thickness after compression $\delta_{sp}=250$ μm). The salt solution flows from outside the stack on all four sides into a square 6x6 cm^2 spacer channel of each of the N cells, and leaves from a hole (1.5x1.5 cm^2) in the middle of each cell (standard value for total stack flow rate $\Phi_{stack}=60$ mL/min). After assembly, all layers in the stack are compressed and placed in a teflon housing. The stack is fed from a 10 liter vessel storing an NaCl-solution as the electrolyte, to which the effluent is recycled. The conductivity of the effluent is measured (not in the storage vessel) on-line and is converted into salt concentration according to a calibration curve. The electric current through the stack is applied using a potentiostat (Iviumstat Standard, Ivium Technologies, The Netherlands) which also measures the cell voltage, V_{cell}. The salt adsorption and charge in an MCDI-cycle can be derived from the data of salt effluent (outflow) concentration versus time, and electric current versus time. For salt adsorption, the difference between inflow salt concentration and outflow concentration is integrated with time, and multiplied with the water flow rate, while for charge, the current is integrated with time. After a few cycles, the dynamic steady state is reached where the measured salt adsorption during one phase of the cycle is close (ideally, equal) to the salt desorption in the other phase of the cycle (salt balance is maintained). Likewise, the total charge transferred in one direction (from cathode to anode) during the salt adsorption step, is close to the charge transfer directed in the opposite direction during the salt release-step. In the standard experiment we apply ±1 A to the full stack of $N=8$ cells, which translates to an average current density (per unit cell area) of ±38.4 A/m^2.

Energy requirements

To calculate the energy requirement for the removal of an ion, as presented in Fig. 4, we take the ratio of energy consumption over desalination, both calculated strictly based on the duration of the ion adsorption step. In the present work, the adsorption step is defined to start and end at the exact moments that voltage or current signals are changed, not by the moments that the effluent salt concentrations drops below, or increases to beyond, the inlet salt concentration (which is 20 mM in Figs. 3 and 4). Desalination is calculated from integration over time, during the ion adsorption step, of the difference $c_{in}-c_{effluent}$, and multiplying by water flow rate Φ, and by the factor 2. The factor 2 is because we present data for the energy to remove an ion, not to remove a salt molecule. The energy is

calculated as cell voltage V_{cell} times current I, integrated again over the duration of the ion adsorption step. The ratio energy/desalination gives us the energy in J per mole of ions removed. Dividing this number by a factor RT (=2.48 kJ/mol at room temperature) results in the energy in units of "RT per mole of ions", which has the same numerical value as when expressed in "kT per ion" as in Fig 5a-c.

Dynamic charge efficiency

The dynamic charge efficiency, Λ_{dyn}, denotes the ratio of two properties: the total desalination during ion adsorption (in moles), as described above, divided by total charge transferred in the same period (charge with unit Coulomb must be divided by Faraday's constant, F, to obtain charge in moles). In the present work, the parameter Λ_{dyn} is obtained during relatively short cycles in which the EDLs are not allowed to come to equilibrium with a well-known salt concentration in the pores next to it. Thus, formally, we have not measured (nor do we theoretically model), the equilibrium charge efficiency, Λ, as defined in refs. [20,21,27,37,38], which requires that the system becomes equilibrated at set values of the cell voltage. Thus, to describe the measured ratio of desalination and charge, in the present work we use the modified term, "dynamic charge efficiency."

Theory

The theoretical model used to describe ion transport and storage in MCDI and CDI is described in detail in refs. 38 and 48. Here we only give the general outline, and present in Table 1 the model input parameters. Previous modeling work related to (M)CDI considered fully-mixed conditions in the spacer channel [21,27], while salt storage was described using the Gouy-Chapman-Stern model which assumes planar non-overlapping electrical double layers (EDLs) within the electrode [20,21,27,43,55-59]. This EDL-model does not consider the difference between the two types of porosity that can be distinguished in typical activated carbon electrodes, namely the macropores (transport pathways) in between the porous activated carbon particles, and the micropores (intraparticle porosity), see Fig. 2. It also does not recognize that within the micropores the EDLs are strongly overlapping. To account for these effects we developed in refs. [38,40,48,56,60] an improved "two-porosity" model which distinguishes between the charge-neutral macropores and the micropores in which the EDLs are formed and counterions are preferentially stored. The EDLs are described using a modified Donnan (mD) model which assumes a constant micropore potential and also includes a non-electrostatic attractive term, μ_{att}, when the ion enters the micropores. In between the ion- and water-filled micropores and the charged carbon walls we assume the presence of a thin dielectric Stern layer. To describe the water flow in the spacer channel along the electrode we model the system by placing a number M of sub-cells in series, see Fig. 2, and refs. [38,43,48]. For details on the theoretical model, we refer the reader to refs. [38,48]. Note that all calculations presented in this work (Figs. 3-5) are based on a single set of parameter values, given in Table 1. A technical modification made in the present work relative to refs. [38,48] is that the Stern layer capacity per unit area is lumped with the area/volume ratio $h_{p,mi}$ to arrive at a volumetric capacity, while additionally we assume $C_{St,vol}$ to be an explicit (weak) function of micropore charge density, and not to depend explicitly on Stern voltage, $\Delta\phi_{St}^2$; thus we use $\Delta\phi_{St} = -F/V_T \cdot c_{charge,mi} / \left(C_{St,vol,0} + \alpha \cdot c_{charge,mi}^2 \right)$ see also refs. [37,40]. Also note that in

most of the experiments presented here we do not apply a constant voltage, but we apply a total current to the whole cell. This total (average) ion current density, I_{tot}, distributes self-consistently over the M sub-cells, thus $I_{tot} = \frac{1}{M}\sum_{i=1}^{M} I_i$ is solved for all M sub-cells simultaneously. In all sub-cells, the cell voltage is at each moment in time the same throughout the electrode. Beyond this modification of the externally applied current-voltage characteristic, there is for the ions no fundamental difference between CV- or CC-operation, in the sense that the forces acting on an ion to move into the pores and to be stored there, are fundamentally unchanged.

Results and Discussion

in this section we show results of MCDI operation using different operational modes, focusing on the difference between constant voltage (CV) and constant current (CC) operation. Results are presented of two modes of CC operation. For these three modes in total, to be discussed below in detail, we show in Fig. 3 experimental and theoretical results for three main operational characteristics: effluent concentration, cell voltage, and current, all as function of time. Note that in all experiments of Fig. 3 the inlet salt concentration is $c_{salt,in}$=20 mM, even though Fig. 3c may suggest otherwise; but note that here the effluent concentration of ~30 mM shown at time zero is not the inlet concentration but the effluent concentration as produced during the previous desorption-step. Furthermore, in all cases (also for Figs. 4 and 5), results are shown of a steady-state cycle, i.e., not the first or second cycle from a new series, but a cycle which repeats itself almost unchanged for a prolonged period. In all nine panels, data are presented as dashed red lines, and predictions of the theoretical model of ref. [48] are shown by solid blue curves.

The three characteristics presented in Fig. 3 are: on the top row, first of all the effluent concentration (the concentration of the freshwater during the first period, denoted "adsorption" in panels a-c, and the concentration of the high-salinity stream in the desorption step); second the cell voltage (middle row; either applied or measured); and finally the electrical current (bottom row; either applied or measured). The first vertical column shows results of classical operation at constant voltage, as used in practically all previous work in the literature of CDI and MCDI. In this case, operation is first for a predetermined duration (here 300 s) at a preset value of the cell voltage, namely V_{cell}=1.2 V (see panel d) to desalinate the water, followed by a stage of the same duration at zero cell voltage. The current (panel g) is high at the start of each step and then decays back to zero. The salt effluent concentration (panel a) shows the minimum during ion adsorption as discussed previously, while during desorption we have a short peak in salt concentration before the concentration slowly decays back to the inlet value.

In the second column we show results of applying constant current (CC) conditions, but in this case CC is only applied during ion adsorption, while the ion desorption step is still defined by applying a zero voltage (now for 500 s; CC-ZVD mode). The CC-condition is applied until a preset upper voltage limit of V_{cell}=1.6 V is reached. At that moment we switch to the desorption step. Because of operation at CC during ion adsorption, the cell voltage steadily increases, after an initial rapid increase due to Ohmic resistances (panel e). Most importantly, we see in panel b that the freshwater salt effluent

concentration is now at a stable value during the ion adsorption step (after a brief initial transition period), here around $c_{freshwater}$=10 mM.

In the third, right, column we show results of CC operation where also during desorption a constant current is applied, of equal magnitude but opposite in sign compared to adsorption (see panel i; CC-RCD mode). Both steps are now defined by limiting values of the cell voltage, being 1.6 V during adsorption and 0 V during desorption. The cell voltage increases relatively linear for most of the time except for brief transition periods where it rapidly changes because of the Ohmic resistances, which we attribute in the theory to ion transport resistances in the spacer channel and in the electrode. Panel c shows the main result, namely that using CC operation in both steps of the cycle leads to very stable effluent ion concentrations, unvarying in time. Brief initial transition periods are due to the relatively large mixing volumes after the stack in our small laboratory setup.

Fig. 3 has introduced the two novel modes of CC-operation, and shows how using CC-operation we can achieve a stable effluent freshwater salt concentration. Next we show how we can tune this effluent concentration by varying the current I, or the water flow rate Φ. As these are easily adjustable parameters during operation, these are suitable control variables to be adjusted when the setpoint of the system is to be changed, such as the salinity of the produced freshwater, or when we must correct for any gradual losses of performance over prolonged use. Results of these experiments are shown in Fig. 4, where we show the stable effluent concentration in the two steps of the cycle (first part with low effluent concentration is the ion adsorption step; the second part is for ion desorption) as function of current (panel a), and water flow rate (panel c). The duration of the adsorption step is set to 120 s, while the desorption step ends when the cell voltage has returned to V_{cell}=0 V. It can be seen in panels a and c that upon increasing the current or upon decreasing the flowrate (in both cases following the direction of the arrows), the effluent salinity of the freshwater decreases. This is shown in more detail in panels b and d where we show quantitatively the levels of the effluent concentration during adsorption and desorption, as function of current I and flowrate Φ. Fig. 4b shows how the effluent concentration depends linearly on current, while Fig 4d shows that varying the water inlet flowrate Φ by a factor of ~3, allows us to change the effluent freshwater salinity also by a factor of ~3. This makes sense because by reducing the water flow rate by a factor x, the total charge per unit water volume treated in a cycle increases by x and thus, for the same charge efficiency (see below), this will lead to x times more desalination per unit water volume. Fig. 4 shows, both experimentally and theoretically, how we can tune the effluent salt concentration to a desired setpoint, with the expected dependency that higher currents and lower water flow rates both lead to more desalination.

Finally, we show in Fig. 5 a large data set for the energy consumption per mole of ions removed in MCDI, for the three operational modes discussed previously in Fig. 3, as function of operational mode, system layout (with/out membranes), and inflow salt concentration, $c_{salt,in}$. To be able to compare MCDI with CDI, we add here data for CDI. Fig. 5 shows results both of experiments, and of the (M)CDI model of ref. [48]. Note that energy recovery during the ion desorption step, possible in the CC-RCD mode of operation, is not included in this calculation. Analyzing the integral of voltage vs time in Fig. 3f we find that in our experiments the potential for energy recovery is about 40%, which would make the numbers presented in Fig. 5c drop by the same amount. For the experiments reported in Fig. 5, operational

conditions are the same as in Fig. 3, except for the duration of each step in CV, which now is 500 s, and for the fact that now we vary $c_{salt,in}$. We observe that for MCDI a lower limit in energy consumption is found of around 22 kT/ion removed. This value is independent of $c_{salt,in}$ for CC operation, while the energy consumption increases moderately with $c_{salt,in}$ for CV-operation. For CDI, energy consumption is higher than for MCDI, and more dependent on $c_{salt,in}$, especially for CC-operation. Fig. 5 shows in general somewhat lower energy consumption for CC-operation than for CV-operation, but not as dramatic as a simple argument would suggest based on the fact that in CC-operation the average cell voltage is lower; neither is the energy-consumption in CC-operation higher than for CV-operation, which may be inferred in first approximation when considering that with the voltage increasing during the cycle, the energetic penalty for an extra ion to adsorb (for each electron to be tranferred against the growing cell voltage) will increase steadily. Instead we find more subtle differences between the energy requirement in CC- and CV-operation, differences which will depend on the durations of the adsorption- and desorption steps, salt concentration, and chosen voltage and current levels.

To explain, at least partly, the influence of the various variables on energy consumption, we evaluate in the second row of Fig. 5 the dynamic charge efficiency, Λ_{dyn}. This parameter denotes the ratio of two properties: the total desalination during ion adsorption, divided by total charge transferred in that same period. For technical details of this calculation, see the Experimental Section. In Fig. 5, we observe an almost 1:1 match between the data for Λ_{dyn} and energy consumption, with higher Λ_{dyn} resulting in lower energy consumption.

Finally, quite surprisingly, Fig. 5 shows that the energy consumption does not decrease steadily with increasing salt concentration, which in first approximation would be expected because the ionic resistance in the spacer channel and macropores will decrease with increasing salinity. Instead, we find that for MCDI the energy consumption is fairly independent of salt concentration, while for CDI it even increases with c_{salt}. Though these experimental observations are well reproduced by the theory, as yet, we do not have available a simple argument to rationalize these counterintuitive results.

Conclusions

In conclusion, we have demonstrated that the use of constant electrical current operation in membrane capacitive deionization (MCDI) results in a stable produced freshwater concentration, not varying in time. By tuning the level of the electrical current, or the water flowrate, the freshwater salinity can be accurately adjusted. We present an extensive data set for the energy requirements of water desalination, both for CDI and for MCDI, and both for the constant current (CC) and constant voltage (CV) mode of operation. According to both the data and the theoretical model, in all situations considered, MCDI has lower energy requirements than CDI, and this difference is larger for CC-operation than for CV-operation. This difference correlates with higher dynamic charge efficiency (the ratio of salt adsorption over charge) for MCDI relative to CDI. The theoretical model reproduces most experimental data for MCDI well, though deviations remain, especially for CDI at high ionic strength and CV-operation. Nevertheless, the theoretical model is an essential tool to design and optimize the MCDI system, and for the evaluation of the economic viability of this technology.

References

1. R. Connor, WWAP (World Water Assessment Programme). 2012. *The United Nations World Water Development Report 4: Managing Water under Uncertainty and Risk*. Paris, UNESCO.

2. T.J. Welgemoed and C.F. Schutte, *Desalination*, 2005, **183**, 327.

3. M.A. Shannon, P.W. Bohn, M. Elimelech, J.G. Georgiadis, B.J. Marinas and A.M. Mayes, *Nature*, 2008, **452**, 301.

4. A. Cipollina, *Seawater desalination: conventional and renewable energy processes*, Springer, Berlin, 2009.

5. M. Elimelech and W.A. Phillip, *Science*, 2011, **333**, 712.

6. A. Bajpayee, T. Luo, A. Muto and G. Chen, *Energy Environm. Sci.*, 2011, **4**, 1692.

7. M.M. Pendergast and E.M.V. Hoek*, Energy Environ. Sci.*, 2011, **4**, 1946.

8. H. Strathmann, in: R.W. Baker, *Membrane Separation System: Recent Developments and Future Directions*; Noyes Data Corporation, Park Ridge, NJ., (1991) p. 396.

9. S.J. Kim, S.H. Ko, K.H. Kang and J. Han, *Nat. Nanotechnol.*, 2010, **5**, 297.

10. M. Pasta, C.D. Wessells, Y. Cui and F. La Mantia, *Nano Lett.*, 2012, **12**, 839.

11. C. Forrestal , P. Xu and Z. Ren, *Energy & Environm. Sci.*, 2012, **5**, 7161.

12. S. Porada, B.B. Sales, H.V.M. Hamelers, and P.M. Biesheuvel, *J. Phys. Chem. Lett.*, 2012, **3**, 1613.

13. B.B. Arnold and G.W. Murphy, *J. Phys. Chem.*, 1961, **65**, 135.

14. A.M. Johnson and J. Newman, *J. Electrochem. Soc.*, 1971, **118**, 510.

15. J.C. Farmer, S.M. Bahowick, J.E. Harrar, D.V. Fix, R.E. Martinelli, A.K. Vu and K.L. Carroll, *Energy & Fuels*, 1997, **11**, 337.

16. M.-W. Ryoo and G. Seo, *Water Res.*, 2003, **37**, 1527.

17. D. Qi, L. Zou and E. Hu, *Research Journal of Chemistry and Environment*, 2007, **11**, 92.

18. Y. Oren, *Desalination*, 2008, **228**, 10.

19. P. Xu, J.E. Drewes, D. Heil and G. Wang, *Water Research*, 2008, **42**, 2605.

20. P.M. Biesheuvel, *J. Colloid Interf. Sci.*, 2009, **332**, 258.

21. P.M. Biesheuvel, B. van Limpt and A. van der Wal, *J. Phys. Chem. C*, 2009, **113**, 5636.

22. R. Broséus, J. Cigana, B. Barbeau, C. Daines-Martinez and H. Suty, *Desalination*, 2009, **249**, 217.

23. Y. Bouhadana, E. Avraham, A. Soffer and D. Aurbach, *AIChE J.*, 2009, **56**, 779.

24. L. Pan, X. Wang, Y. Gao, Y. Zhang, Y. Chen and Z. Sun, *Desalination*, 2009, **244**, 139.

25. S. Nadakatti, M. Tendulkar and M. Kadam, *Desalination*, 2010, **268**, 182.

26. M. Wang, Z.-H. Huang, L. Wang, M.-X. Wang, F. Kang and H. Hou, *New J. Chem.*, 2010, **34**, 1843.

27. R. Zhao, P.M. Biesheuvel, H. Miedema, H. Bruning and A. van der Wal, *J. Phys. Chem. Lett.*, 2010, **1**, 205.

28. J.-H. Lee, W.-S. Bae and J.-H. Choi, *Desalination*, 2010, **258**, 159.

29. R.T. Mayes, C. Tsouris, J.O. Kiggans Jr, S.M. Mahurin, D.W. DePaoli and S. Dai, *J. Mater. Chem.*, 2010, **20**, 8674.

30. Y. Bouhadana, E. Avraham, A. Soffer and D. Aurbach, *AIChE J.*, 2010, **56**, 779.

31. H. Li, L. Pan, Y. Zhang, L. Zou, C. Sun, Y. Zhan and Z. Sun, *Chem. Phys. Lett.*, 2010, **485**, 161.

32. S.-J. Seo, H. Jeon, J.K. Lee, G.-Y. Kim, D. Park, H. Nojima, J. Lee and S.-H. Moon, *Water Res.*, 2010, **44**, 2267.

33. M.A. Anderson, A.L. Cudero and J. Palma, *Electrochimica Acta*, 2010, **55**, 3845.

34. J. Yang, L.D. Zou, H.H. Song and Z.P. Hao, *Desalination*, 2011, **276**, 199.

35. B.G. Jeon, H.C. No and J.I. Lee, *Desalination*, 2011, **274**, 226.

36. Z.-H. Huang, M. Wang, L. Wang and F. Kang, *Langmuir*, 2012, **28**, 5079.

37. S. Porada, L. Weinstein, R. Dash, A. van der Wal, M. Bryjak, Y. Gogotsi and P.M. Biesheuvel, *ACS Appl. Mat. & Interf.*, 2012, **4**, 1194.

38. S. Porada, M. Bryjak, A. van der Wal and P.M. Biesheuvel, *Electrochimica Acta*, 2012, **75**, 148.

39. G. Wang, C. Pan, L. Wang, Q. Dong, C. Yu, Z Zhao and J Qiu, *Electrochimica Acta*, 2012, **69**, 65.

40. R. Zhao, M. van Soestbergen, H.H.M. Rijnaarts, A. van der Wal, M.Z. Bazant and P.M. Biesheuvel, *J. Colloid Interface Sci.* (2012). DOI: http://dx.doi.org/10.1016/j.jcis.2012.06.022

41. J.-B. Lee, K.-K. Park, H.-M. Eum and C.-W. Lee, *Desalination*, 2006, **196**, 125.

42. H. Li, Y. Gao, L. Pan, Y. Zhang, Y. Chen and Z. Sun, *Water Res.*, 2008, **42**, 4923.

43. P.M. Biesheuvel and A. van der Wal, *J. Membr. Sci.*, 2009, **346**, 256.

44. Y.-J. Kim, J. Hur, W. Bae and J.-H. Choi, *Desalination*, 2010, **253**, 119.

45. Y.-J. Kim and J.-H. Choi, *Water Res.*, 2010, **44**, 990.

46. J.-Y. Lee, S.-J. Seo, S.-H. Yun and S.-H. Moon, *Water Res.*, 2011, **45**, 5375.

47. M. Andelman, *Sep. & Purif. Techn.*, 2011, **80**, 262.

48. P.M. Biesheuvel, R. Zhao, S. Porada and A. van der Wal, *J. Colloid Interf. Sci.*, 2011, **361**, 239.

49. H. Li and L. Zou, *Desalination*, 2011, **275**, 62.

50. M.E. Suss, Th. Baumann, B. Bourcier, Ch. Spadaccini, K.A. Rose, J.G. Santiago, and M. Stadermann, *Energy Environ. Sci.*, 2012, **x**, DOI: http://dx.doi.org/10.1039/C2EE21498A

51. J. Biener, M. Stadermann, M. Suss, M.A. Worsley, M.M. Biener, K.A. Rose and Th.F. Baumann, *Energy Environ. Sci.*, 2011, **4**, 656.

52. Y Hou, R. Vidu and P. Stroeve, *Ind. Eng. Chem. Res.*, 2011, **50**, 8954.

53. S. Kondrat, V. Presser, C.R. Perez, Y. Gogotsi and A.A. Kornyshev, *Energy Environm. Sci.*, 2012, **5**, 6474.

54. S.Sigalov, M.D. Levi, G. Salitra, D. Aurbach, and J. Maier, *Electrochem. Comm.* 2010, **12**, 1718.

55. P.M. Biesheuvel and M.Z. Bazant, *Phys. Rev. E*, 2010, **81**, 031502.

56. P.M. Biesheuvel, Y. Fu and M.Z. Bazant, *Phys. Rev. E*, 2011, **83**, 061507.

57. B.B. Sales, M. Saakes, J.W. Post, C.J.N. Buisman, P.M. Biesheuvel, H.V.M. Hamelers, *Environ. Sci. Technol.,* 2010, **44**, 5661.

58. D. Brogioli, R. Zhao and P.M. Biesheuvel, *Energy Environm. Sci.*, 2011, **4**, 772.

59. N. Boon and R. van Roij, *Mol. Phys.*, 2011, **109**, 1229.

60. P.M. Biesheuvel, Y. Fu and M.Z. Bazant, *Russ. J. Electrochem*, 2012, **48**, 580.
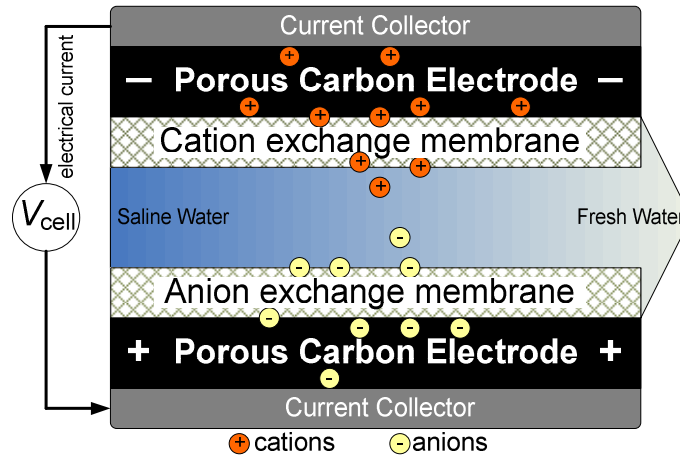
Fig. 1. Schematic view of a Membrane Capacitive Deionization-cell. By applying an electrical field, cations in the water flowing through the spacer channel migrate through the cation exchange membrane and are stored inside the adjacent porous carbon electrode (cathode) while anions are stored in the opposite electrode (anode). As a consequence, the water flowing through the cell is desalinated.
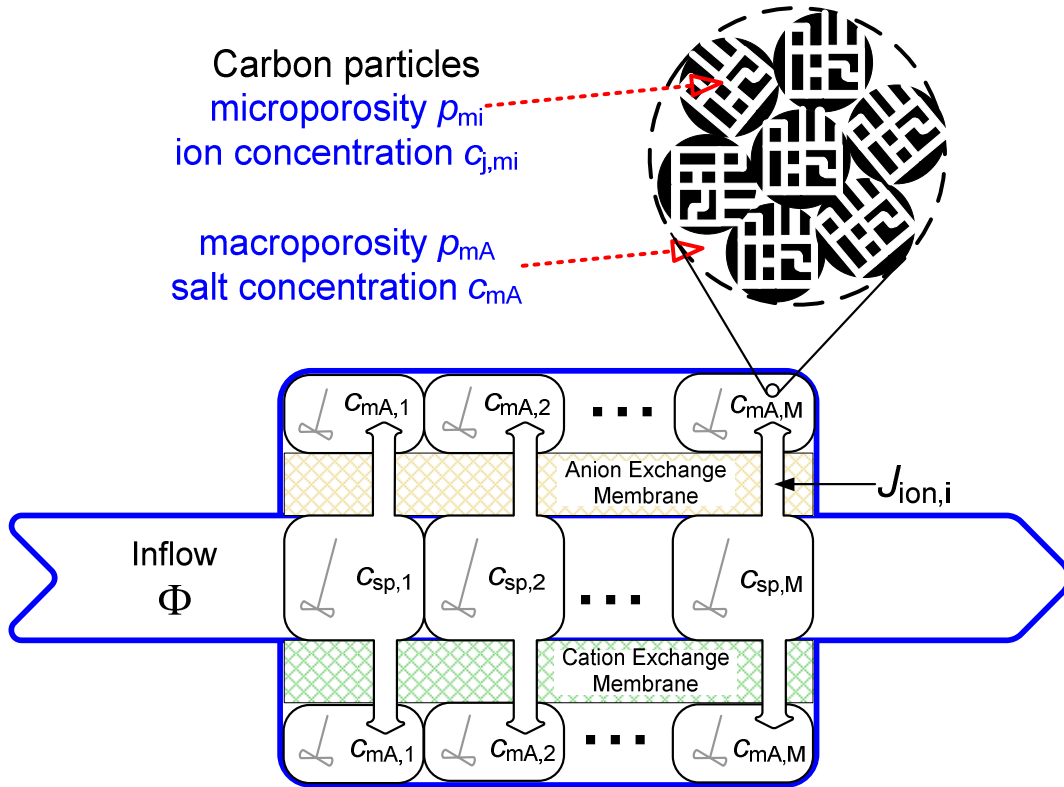
Fig. 2. Schematic view of MCDI model for ion transport and storage. Here, $J_{ion,i}$ is the ion flux from the spacer channel into the electrode in each of the i=1..M sequential sub-cells. The electrode contains both macropores and micropores. In the macropores cat- and anions have the same concentration c_{mA}, while in the micropores the difference between cation and anion number is compensated by electronic charge present in the carbon matrix.
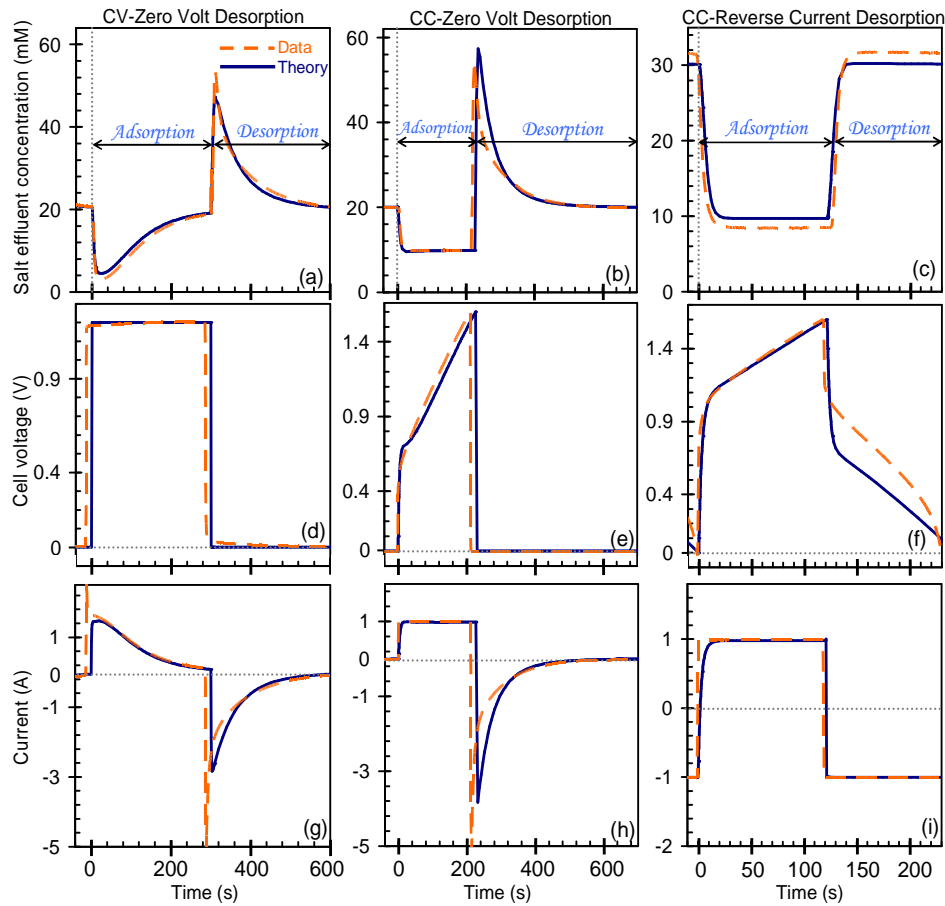
Fig. 3. Comparison of three operational modes of MCDI: constant voltage (CV, left column); constant current during adsorption (CC) with zero voltage during desorption (ZVD, middle column); and CC with reverse current during desorption (RCD, right column). Shown are results for effluent salt concentration (top row), cell voltage (middle row), and current (bottom row), as function of time, for one cycle. Inlet salt concentration: $c_{salt,in}$=20 mM. In the CV-mode we have adsorption at V_{cell}=1.2 V and desorption at V_{cell}=0 V (both steps have a duration of 300 s); in CC-ZVD we have salt adsorption at +1 A until V_{cell}=1.6 V, while during desorption V_{cell}=0 V for 500 s; in CC-RCD desorption is controlled by a current of -1 A until the voltage is back at 0 V. Solid blue lines: theoretical simulations, dashed red lines: experimental data.
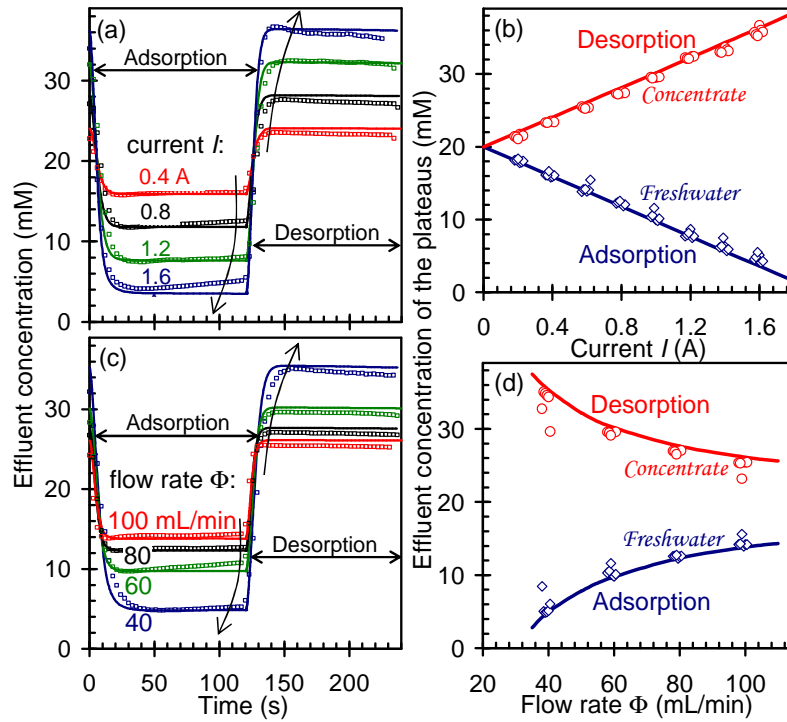
Fig. 4. Control of effluent concentration of freshwater and concentrate in MCDI-CC-RCD mode, using as control variable: (a) Electrical current, I, and (b) Water flow rate, Φ. The same magnitude of the current is used during ion adsorption (first 120 s), as during ion desorption (second period of ~120 s). Inlet salt concentration $c_{salt,in}=20$ mM. In (a,b) water flow rate $\Phi=60$ mL/min; in (c,d) current ±1 A. Lines are based on theory, and data are shown as symbols. Arrows point in direction of higher desalination degree.
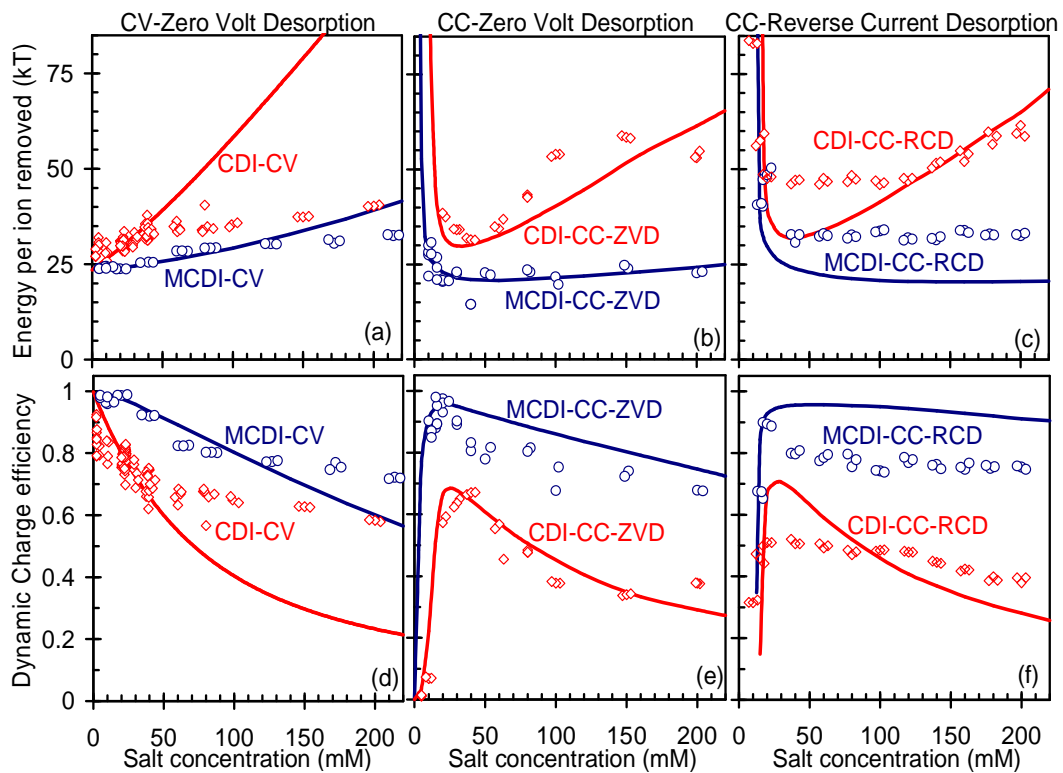
Fig. 5. Energy consumption and dynamic charge efficiency in CDI and MCDI. Comparison of same three operational modes as in Fig. 3, but now as function of the inlet salt concentration, $c_{salt,in}$. For other parameter settings, see main text and Fig. 3. Panels a-c show the the energy requirement per ion removed, and panels d-f show the dynamic charge efficiency, Λ_{dyn}, being the ratio of the salt adsorption vs charge. In all panels, lines are theory and points are data.

p_{mA}, p_{mi}	electrode macroporosity, microporosity	30, 30	%	*
δ	thickness of spacer, membrane, electrode	250,140,362	μm	*
X	ion exchange capacity of the membrane	3000	mol/m^3	-
D	ion diffusion coefficient in the spacer channel	$1.68 \cdot 10^{-9}$	m^2/s	-
D_{mem}	ion diffusion coefficient in the membrane	$1.12 \cdot 10^{-9}$	m^2/s	-
$C_{St,vol,0}$	Stern layer capacitance at zero charge	0.12	GF/m^3	*
α	parameter to describe non-linear Stern capacity	17.3	F$\cdot$m^3/mol^2	-
R_{elec}	specific electrode resistance	0.12	$\Omega\cdot$mol/m	*
	fraction of total flow going through one electrode	1	%	-
μ_{att}	chemical attraction term between ions and carbon	1.4	kT	*
M	number of sequential sub-cells in the model	6		*

Table 1. Parameter settings for MCDI transport model. (*/- same/different compared to ref. [48]).

Graphical Abstract